Journal Name

ARTICLE

A simple procedure for the production of large ferromagnetic cobalt nanoparticles

Received 00th January 20xx,
Accepted 00th January 20xx

DOI: 10.1039/x0xx00000x

www.rsc.org/

Rebecca O. Fuller,*[a] Bee-Min Goh, [a] George. A. Koutsantonis, [a] Matthys J. Loedolff, [a] Martin Saunders,[b] and Robert C. Woodward[c]

Epsilon cobalt (ε-Co) nanoparticles in a number of octahedral morphologies have been synthesised. The particles are polycrystalline, with sizes in the order of 30 nm. Magnetic studies reveal the particles are ferromagnetic, with a room temperature saturation magnetisation of 131 emu/g. Unlike other large cubic ε-Co syntheses, we have not added an additional co-surfactant. Instead, we have modified the heating regime and reaction agitation. This alternative method highlights the complex chemistry associated with the formation of cobalt nanoparticles by thermal decomposition.

Introduction

Magnetic nanoparticles are an area of intense scientific research due to their potential application in catalysis,[1, 2] information storage,[3] sensing[4] and medicine.[5-8] In addition to elemental composition, the magnetic properties of a particle are intrinsically linked to the particle size, crystalline structure and shape. Although colloidal systems have been available for some time, it wasn't until more recently that advances in the production of high quality magnetic nanoparticles with tunable shape, size and composition were achieved.[5, 9, 10] Methodologies for producing magnetic particles with sizes < 20 nm are well established.[3] These smaller nanoparticles are generally superparamagnetic. Although larger ferromagnetic particles are often desirable for applications, [11] such as magnetically induced heating,[12] only a handful of such systems comprised of larger single domain nanoparticles in the 30-100 nm range have been made.[13-16]

Since the late 1990s significant progress has been made in the synthesis of monodisperse magnetic systems containing iron, cobalt and nickel. Cobalt nanoparticles can be formed by high temperature thermal reduction of $Co_2(CO)_8$ or $CoCl_2$ in the presence of oleic acid and trioctylphosphine oxide. Like other nanoparticles produced by high temperature methods, the cobalt particles produced by this method, are monodisperse and single crystal. The high quality particles are spherical and in an epsilon phase. Sizes can be tuned to be in the 2-15 nm range.[10, 17] Modification of the heating regime and addition of a co-surfactant to the reaction has led to the production of *hcp*-Co nanodisks, [18] and larger spherical particles (~20 nm) that were not stable in air at room temperature.[19] Co nanorods have also been produced from the use of more exotic organometallic precursors with high pressure.[20, 21] A number of larger cubic cobalt nanoparticles with sizes > 20 nm have been produced with the use of additional surfactants to the thermal decomposition.[16, 22, 23]

Large cobalt particle systems have been developed for a number of magnetic applications including those based on exchange bias. Cobalt nanoparticles readily undergo surface oxidation on exposure to air.[24] The spontaneous oxidation results in the formation of a CoO layer some 1-2 nm in thickness. CoO layers of an adequate thickness can alter the magnetic properties of the particles. [24] Exchange bias (EB) is a type of magnetic coupling that occurs at the interface of the ferromagnetic (Co core) and antiferromagnetic (CoO layer) material. EB can be used to control the coercivity of a material. Materials with exchange bias are being developed for a range of applications including magnetic sensing and a way to improve the superparamagnetic limit of nanoparticles. [25, 26]

Although high temperature synthetic methods for the production of high quality cobalt nanoparticles have been known for almost two decades,[10] the system is still not as fully developed as many of the other colloid systems made using this method. This perhaps is the result of the chemistry of cobalt nanoparticles being more complex. Experimentally, synthetic routes to larger sizes and alternative shapes are still

[a] School of Chemistry and Biochemistry M310, The University of Western Australia, Crawley WA 6009, Australia. Email: rebecca.fuller@uwa.edu.au
[b] Centre for Microscopy, Characterisation and Analysis, M010, The University of Western Australia, Crawley WA 6009, Australia.
[c] School of Physics, M013, The University of Western Australia, Crawley WA 6009, Australia.

Electronic Supplementary Information (ESI) available: [TEM imaging and reaction conditions (Figure S1 and Table S1) for three repeat reactions were large particles are subsequently isolated; a histogram of particle size and example EDX spectrum (Figure S2); TEM imaging and reaction conditions (Figure S3 and Table S2) for three repeat reactions; a full comparison of measured and literature d-spacings (Table S3); a bright field TEM images of a reaction left for t > 20 min (Figure S4); bright field TEM, HRTEM and HAADF STEM images of the reaction at 3 and 6 min (Figure S5) and the product from a reaction with a higher oleic acid content (Figure S6).]. See DOI: 10.1039/x0xx00000x

to be fully realised for cobalt, whereas for metals such as platinum more systematic approaches are available.[27] The synthesis of cobalt nanoparticles, is in part, complicated by the availability of multiple cobalt phases, which are close in energy.[28, 29] Hence, subtle changes in the temperature or surfactant during precursor decomposition can lead to dramatic changes in the particles produced.[18, 30, 31]

To achieve monodisperse particles a short nucleation event followed by a slower period of growth is required along with careful consideration of precursors, solvent, surfactant and heating regime. [32] In the case of cobalt particles three different growth pathways are possible depending on the concentration of the nuclei and surfactants. [11, 13, 19] One of the most widely used procedures for the synthesis of spherical ε-Co involves hot injection of $Co_2(CO)_8$ into oleic acid and trioctylphosphine oxide in dichlorobenzene. Particle size does not significantly increase past 10 nm, even if long reaction times are used. This is a result of the cobalt mononuclear complexes formed from the decomposition of the precursor being exhausted and the nanoparticles are sufficiently stabilised by the surfactant so that no new mononuclear complexes are created to allow further growth.[19] To date, most groups have modified the surfactant system used in the thermal decomposition to achieve different cobalt morphologies. However, the surfactant system for cobalt is complex; the results from additions to it are not always predictable.

The role of the surfactant in a reaction is not only to prevent agglomeration and the passive oxidation of the particles. But the surfactant also significantly impacts of the growth of the particle, namely the resultant crystalinity, shape and size. Generally, using a single surfactant for the production of spherical particles is optimal, due to a minimisation of the surface area.[33] For ε-Co particles, uniform shape and size is only achieved if both trioctylphosphine oxide and oleic acid are used. [18] The use of the second surfactant is essential to improving particle monodispersity, by promoting atom exchange between particles. The addition of a second surfactant is often used to control particle growth along particular crystal faces for a range of other nanoparticle systems.[34] However minor modifications to the surfactant system used in the cobalt octacarbonyl thermal decomposition reaction has been shown to drastically change particle morphology.[19, 31]

The addition of a new surfactant system to a reaction is complex. Particle growth is altered by how strongly the surfactant functional group adheres to the particle surface. Surfactant chains have different diffusion rates, which alter the monomer activity and concentration. The use of ionic additives has been used successfully to prepare large cubic cobalt nanoparticles. [22] However the results are complex and the role of the varying mixtures of organic acids and amines are not well understood. Slight changes to these procedures can drastically alter the outcome. It is highly desirable to develop a more simplified approach to producing these materials.

This investigation came about as the result of our attempts to produce small (5 nm) high quality ε-Co nanoparticles.[31] Curiously, we found that when synthesising high quality single crystal 4.8 ± 0.7 nm ε-Co nanoparticles (Supporting Information Figure S1) using a literature procedure,[31] large ε-Co (36 ± 6 nm) particles also formed as a byproduct.[31] The literature procedure involves[31] maintaining temperature below reflux, ca. 130 °C following the hot injection of $Co_2(CO)_8$ into dichlorobenzene in the presence of oleic acid and trioctylphosphine oxide. This reduction in reaction temperature resulted in greater monodispersity of ε-Co spheres (9.5 nm). [31] In our hands, this procedure has a poor yield (20-30 mg) of high quality single crystal ε-Co particles after 20 minutes reaction time. Following removal of the supernatant with the suspended ε-Co particles, a significant amount of black material (~100 mg) was found attracted to the magnetic stirrer bar. This secondary product could be recovered, by placing the bar into a solvent and applying a second magnetic field. Once particles were attracted to the second magnetic source the stirrer bar was removed from the solution. Particle suspension can be aided by the addition of tridecanol to the solution following removal of the field. Bright field TEM of the material recovered from the bar revealed large polycrystalline ε-Co nanoparticles with an octahedral morphology and a size of the order of 36 ± 6 nm (Supporting Information Figure S1). Although the stirrer bar allows easy recovery of these large nanocrystallites and the reaction produces a significant amount of product (100 mg), we have, in this work, modified the literature ε-Co synthetic procedure to exclusively form the larger size polycrystalline epsilon cobalt nanoparticles. We have explored methods based on changes to the heating regime and diffusion of reactants rather than altering the surfactant system. Our synthetic procedure is different to the other reported methods for producing cobalt nanoparticles of this size and shape, [16, 22, 23] in that only oleic acid and trioctylphosphine oxide are used as surfactants. The particle morphology is controlled by modification of the temperature, rate of agitation and surfactant concentration.

Experimental

Synthesis, post reaction processing and storage of large, cubic cobalt nanocrystals were carried out under argon using standard Schlenk conditions. Reagents and solvents include: Octacarbonyldicobalt (Strem, recrystallised from hexane); trioctylphosphine oxide (TOPO) (Sigma Aldich 99 %); oleic acid (OA) (Sigma Aldrich 90 %); 1,2-dichlorobenzene (DCB) (Sigma Aldrich distilled CaH_2 or anhydrous 99 %).

The synthesis involved the modification of literature procedures developed for the production of small spherical single crystal ε-Co particles.[30, 31, 35, 36] A typical reaction involved a 1,2-dichlorbenzene solution (3-4 mL) of $Co_2(CO)_8$ (0.54 g, 1.58 mmol) being heated to 50 °C then injected into a mixture containing trioctylphosphine oxide (0.1 g, 0.25 mmol), oleic acid (0.2 mL, 0.63 mmol) in 15 mL 1,2-dichlorobenzene at

reflux. The solution was not stirred. Following the hot injection the temperature of the solution drops and was maintained at 120-140 ^{O}C for 20 min. After which, the solution is cooled under a flow of argon and then transferred to a flask where 50 mL methanol is added. The temperature range reflects the variation that occurs in different reactions following the hot injection process. The nanoparticles will settle out over 8 hours but the settling time can be decreased to around 4 hours through application of a magnetic field gradient. Solvent is then removed under vacuum. Particles (~100 mg) are stored under Ar as either a solid or as a suspension in hexane. Tridecanol can be added (5-20 mg) to hexane to aid suspension following methanol treatment.

Nanocrystal size, morphology, structure and shape were analysed using transmission electron microscopy (TEM). Three microscopes were used; a JEOL 3000F operating at 300 kV, JEOL 2100 operating at 200 kV and a FEI Titan G2 operating at 200 kV. Compositional analysis in the TEM was performed using energy dispersive X-ray (EDX) spectroscopy (Oxford Instruments, JEOL 3000F). Samples were prepared in air by the evaporation of particles suspended in hexane or DCB onto a continuous carbon coated copper grid. Powder X-ray diffraction (XRD) patterns were recorded at room temperature on a Panalytical Empyrean X-ray diffractometer with CuKα radiation generated at 40 kV and 40 mA (step size 0.013^{o} 2θ).

Characterisation of the magnetic properties was carried out using a quantum design MPMS-7 SQUID magnetometer. A small amount (~ 5 mg) of solid was transferred in air to a gelatin capsule. Hysteresis loops in fields up to 7 T were measured at 300 K and at 5 K. The low temperature hysteresis loops were obtained following field cooling from 350 K in a 7 T field. Inductively coupled plasma atomic emission spectroscopy was used to evaluate the Co content of the nanoparticles used in the measurements.

Results and discussion

Hot injection of $Co_2(CO)_8$ into DCB in the presence of OA and TOPO is a well-established procedure for producing spherical, monodispersed ε-Co nanoparticles that are normally <10 nm.[30, 31, 35, 36] The low yields we obtained from using the low temperature production of monodispersed ε-Co prompted us to investigate the nature of the major product. Bright Field TEM images revealed large 36 ± 6 nm octahedral cobalt particles. Micrographs (Figure S1) of the product recovered from the stirrer bar and solution and the reaction conditions (Table S1) are contained in the Supporting Information. We have found that through further minor modifications of the synthetic procedure, viz. to reaction temperature and a lack of agitation resulted in the exclusive formation of larger particles with an octahedral morphology (Fig. 1) and edge length 30 ± 5 nm, an average of a number of particles (Supporting Information Figure S2). The results for three repeat reactions are contained in the Supporting Information (Figures S3 and Table S2). The particles are polycrystalline (individual crystallite size 5-10 nm) and the grain boundaries are evident in high resolution (HR)TEM images. As seen in other cobalt nanoparticles,[19] a 1-2 nm oxide layer is also evident in the HRTEM images, the composition is confirmed by XRD (below). The Fast Fourier Transform (FFT) of the particle in the HRTEM image (Fig. 1d) has discontinuous rings of spots confirming more than one crystal orientation is present in the particle. A series of TEM images where the sample is tilted through 60 degrees (Fig. 2) was used to confirm that the sample was not comprised of the large nanodisks seen by others. [18] In this work the large cobalt particles are octahedral in shape.

The ε-Co phase has been assigned to the particles using powder XRD, Selected Area Electron Diffraction (SAED) and a Fast Fourier Transform (FFT) of HRTEM image (Fig. 3). The peaks in the XRD pattern can be assigned to ε-Co, [17, 37] CoO (JCPDS 09-0402) and Co_2P (JCPDS 89-3030). The occurrence of small peaks in the XRD pattern that can be attributed to CoO is unsurprising, as cobalt nanoparticles are well known to undergo passive (or spontaneous) oxidation on exposure to air.[38] There is a single peak with a *d*-spacing (0.225 nm) suggestive of the Co_2P (JCPDS 89-3030) that has been seen in other cobalt nanoparticles.[39, 40] The SAED and FFT patterns were found to have additional d-spacing's to those previously reported for ε-Co from XRD.[17] Electron diffraction and HRTEM data provide a more complete set of planar spacings than previously reported using XRD[17, 37] as they reveal planes that are weakly scattering or notionally forbidden in the x-ray case. To obtain a full set of *d*-spacings for the ε-Co phase the JEMS software package[41] was used in conjunction with the fractional atomic coordinates of the ε-Co phase.[17] Both the SAED and FFT d-spacings support the nanocrystals occurring in the epsilon phase. A full list of the SAED and XRD d-spacings can be found in the Supporting Information (Table S3). The FFT pattern from

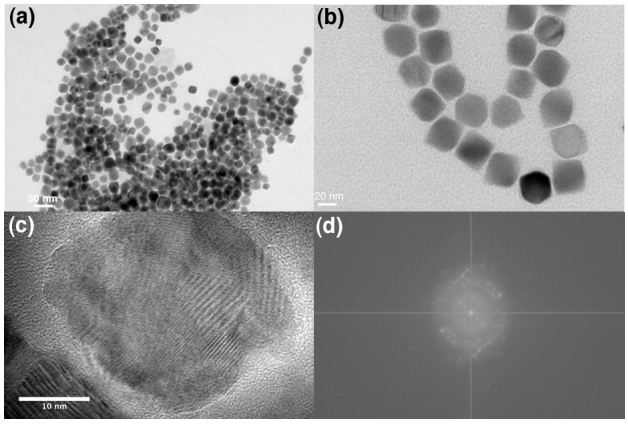

Fig. 1 Bright field TEM images (a-c) of the Co nanocrystals. An FFT (d) of the particle in HRTEM image (c) highlights the polycrystalline nature of the particles .

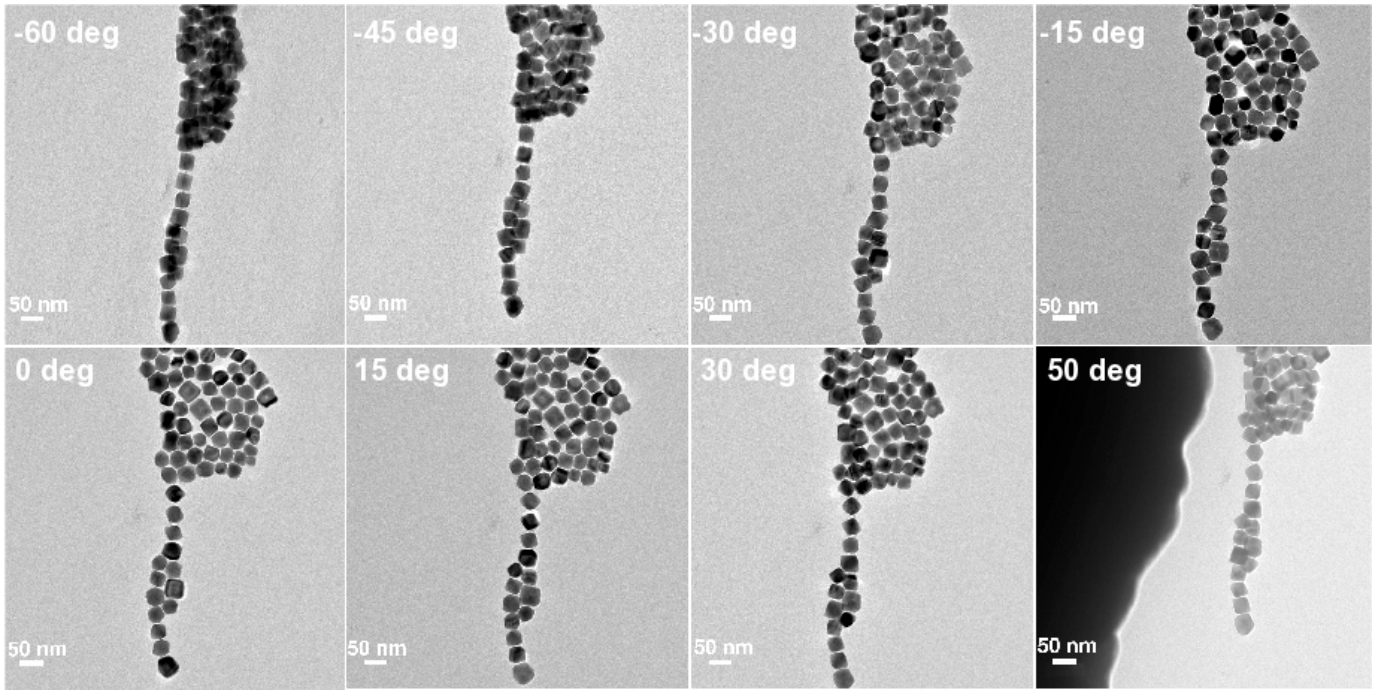

Fig 2 A bright field TEM tilt series of the particles highlights that the particles occur in a number of octahedral morphologies. The tilt level of the grid is indicated.

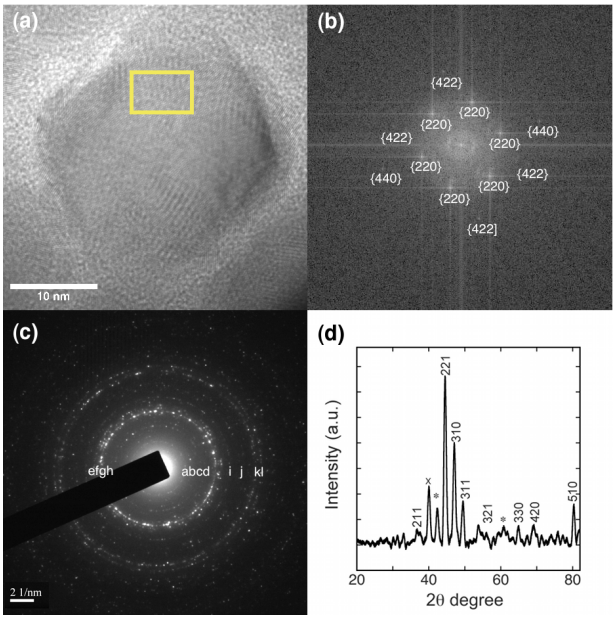

Fig. 3 (a) HRTEM image with FFT area shown; (b) Fast Fourier Transform of (a). The ~0.21 nm {220}, ~0.12 nm {422} and ~0.11 nm {440} *d*-spacings are labelled; (c) Selected area electron diffraction pattern; the labels correspond to the following ε-Co, {hkl}: a {110}, b{111}, c{210}, d{211}, e{220}, f{221}, g{310}, h{311}, i{320}, j{330}, k{510} and l{520}; (e) XRD pattern with ε-Co labelled with Miller indices, for the set of lattice planes responsible for that diffraction peak. The * peaks correspond to the CoO {200} and {220} planes and the x corresponds to Co_2P {112}. Table S3 (Supporting Information) contains the d-spacing for each of the above spectra.

a single crystallite within a polycrystalline particle is shown in Fig. 3b with the principle spots corresponding to the following interplanar distances: ~0.21 nm {220}, ~0.12 nm [1] and ~0.11 nm {440}. This is fully consistent the [111] zone axis of ε-Co phase and inconsistent with those of *hcp*-Co or *fcc*-Co.

The M vs H measurements at both 300 and 5 K are contained in Fig. 4. The particles are ferromagnetic, with a saturation magnetisation, M_s of 140 emu/g (5 K) and 131 emu/g (300 K), which is approximately 80 % of the bulk value for Co (166 emu/g).[42, 43] The reduction in M_s is a result of the formation of the CoO shell around the nanoparticles, which based on the reduced magnetisation should be around 1.5 to 2 nm in thickness. This is consistent with HRTEM observations. We found, after 6 months of further exposure to air, the M_s for the particles (results not shown) only decreased by approximately 5 %, showing that the CoO layer is self-protective and does not continue to significantly thicken after longer exposure to air. [25]

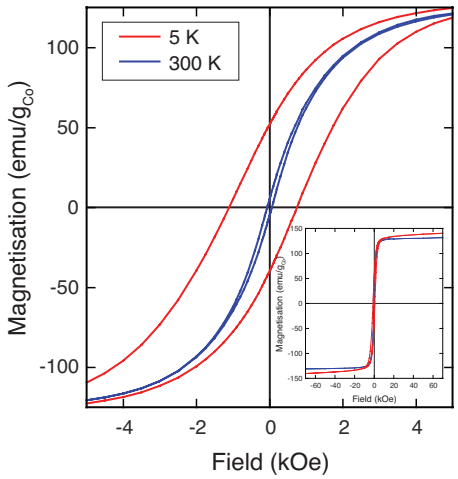

Fig. 4 The M vs H at 300 K (blue) and 5 K (red).

The coercivity at 300 K (~ 60 Oe) is significantly less than would be expected for 30 nm metallic cobalt particles, which would be expected to have relatively high coercivity > 500 Oe. However the higher symmetry of the ε-Co phase means that this phase is considered relatively soft [23, 29] despite only a marginally lower magnetocrystalline anisotropy than the hcp cobalt phase.[29] In addition, the 30 nm particles are not single crystal but polycrystalline and hence consist of randomly orientated smaller crystallites. As such, its effective anisotropy is likely to be further reduced via exchange softening, as seen in nano-crystalline soft magnetic materials.[44, 45] The 5 K results contain a horizontally shifted hysteresis loop with an exchange bias field of around 100 Oe and an enhanced coercivity of 900 Oe, which is above what would be expected for pure ε-Co particles. The enhanced coercivity and shifted loop are the result of exchange bias between the ε-Co particles and the antiferromagnetic CoO layer around the particles.[46, 47]

Traditionally, cobalt nanoparticles formed using hot injection of $Co_2(CO)_8$ into DCB with OA and TOPO has resulted in ε-Co particles that are <10 nm in diameter. In order to produce larger cobalt particles co-surfactants have been added to the reaction. We have developed an alternative that precludes the step of returning the reaction to reflux post injection of the metal precursor and agitation of the solution. We find that if a lower temperature is maintained, the polycrystalline nanoparticles are stable for some 15-20 min. Continuation of the reaction past 30 min leads to the formation of a significant amount of smaller (~2 nm) spherical particles of ε-Co particles (Supporting Information Figure S4).

Nanoparticle growth can be influenced by a range of factors, including surfactant precursor salt and heating regime.[32] Others[13] have shown that larger cubic magnetite particles can be produced by relatively minor changes to the methods developed to synthesis small monodisperse iron oxide nano particles.[48, 49] In particular high monomer concentration and kinetic control were thought to be responsible for the growth of the larger cubic nanocrystallites. Cobalt is known to be a synthetically challenging nanoparticle system.[18] Subtle changes to the synthetic procedure can lead to dramatic changes in the nanocrystals formed. The complexities in Co nanoparticle production can be attributed to the similar energies of the various crystalline phases (hcp, fcc, eplison) of Co[18, 22] and the two-component surfactant system essential for achieving particle monodispersity.

To date others have used additional surfactants to form larger cubic cobalt nanoparticles.[22] However, the mechanisms associated with ionic additives are complex and not well understood for the cobalt system. Hence we have chosen to provide a simpler route for the production of these particles. In particular, we alter the energetics of the reaction by lowering the temperature and reducing agitation. Elevated temperatures used in these reactions are not only for the thermal decomposition of the metal precursor but for atom diffusion and phase transition.[18, 30] The lower temperatures result in a more uniform growth of particles by the Ostwald ripening process.[31] The lack of agitation, also alters the rate of diffusion of the monomers to the surface of the nuclei. This result has also been seen for thermal decomposition reactions of $Co_2(CO)_8$ with TOPO, OA in DCB using higher reaction temperatures and oleyl amine to stabilise the larger particles.[22] Dreyer et al. found the application of a magnetic field induced a shape change of the cobalt particles from cubes to discs with this surfactant system and higher temperature. We add to this result and find that the larger cubic particles can be stabilised and isolated in the presence of a magnetic field as long as a lower reaction temperature is maintained.

To gain further insight into how these larger particles form we have sampled the reaction mixture at 3, 6, 9 and 12 min (Supporting Information Figure S5). The TEM images reveal that only small crystallites are present in the solution at the early reaction times. A few larger nanocrystals (15-20 nm) are observed in TEM images from samples taken at 12 min. HRTEM imaging (Fig. 1c) revealed that the small crystallites are at least 5 nm before fusing takes place. Hence it is unsurprising that we only observe very small single crystals (< 4 nm) when the reaction mixture is imaged at 3 and 6 mins. The size of particle is a function of time, like others our particles are around 5 - 6 nm at ~10 min.[19, 31] Under our conditions once the critical particle size is reached the small crystallites fuse together and form the larger polycrystalline particles. Indeed, we observed the first polycrystalline particles in TEM images at 12 min. Since at 18 min the reaction mixture is predominantly comprised of the larger particles, we believe that there is some critical point at which the smaller single crystals coalesce into larger particles. We also note that if the reaction is not promptly quenched after this event then unreacted cobalt clusters in solution form new nanocrystals. TEM imaging of a reaction continued to 30 min (Supporting Information Figure S4) revealed a significant amount of 2 nm ε-Co particles in addition to the larger polycrystalline particles. ε-Co nanoparticles do not achieve significant growth from 15-30 min.[19] Once the small crystallites fuse, it is no longer

favourable for the unreacted cobalt cluster complexes in solution to be used in the Ostwald ripening growth of the larger particles. The growth equilibrium is shifted and the Co-surfactant complexes form new particles.

The lower temperatures and lack of agitation in our methodology does not support the continued growth of single crystal ε-Co particles. It seems likely that the diffusion growth pathway is modified. Surfactant concentration also plays a significant role in the growth of particles. Oleic acid is known to bind strongly to cobalt. Increasing the concentration of oleic acid in solution stabilises cobalt clusters preferentially to nanocrystals.[31] By slightly increasing the amount of oleic acid in the reaction mixture (0.25 mL) while keeping all other conditions the large polycrystalline Co particles are no longer formed (Supporting Information Figure S6). Increasing the concentration of oleic acid in the solution will in turn increase number of cobalt-surfactant clusters in solution. This is found to stabilise the smaller ε-Co nanocrystals. Perhaps the fusing of the smaller particles is the result of a lower concentration of cobalt-surfactant clusters. A lower surfactant concentration is essential to allowing the coalescence of the smaller crystallites into larger polycrystalline particles.

There has been a vigorous debate in the literature[50] on the shape and size control during the growth of nanoparticles. The resultant particles in this work are not aggregates of smaller nanoparticles rather polycrystallites, comprised of a number of small crystallites with grain boundaries between them. Single crystal cubic (~50 nm) particles of ε-Co and *hcp*-Co have been grown using a polyetheramine.[16] One can envisage that the use of this surfactant could possibly result in micelle formation, physically altering the particle growth by restricting access to the particle surface. When oleyl amine is used as a co-surfactant for the production of larger cubic ε-Co nanoparticles, a different growth mechanism appears to be prevalent as the particles are no longer single crystals.[22] The oleyl amine appears more likely to have absorbed onto the nuclei and regulated growth and the rate at which the Co monomer diffuses to the nuclei being affected by the molecules that are absorbed onto the surface. However, in this work the lower reaction temperature, concentration of OA and lack of agitation of the reaction led to the fusing of the small crystallites into larger polycrystalline particles.

Conclusions

Large cobalt particles could play a key role in future technological developments due to the thermal stabilisation of the magnetisation. Unlike the smaller sized cobalt nanoparticles, these ferromagnetic particles are no longer subject to temperature dependent fluctuations of the magnetisation over time. We have shown that large polycrystalline 30 nm cobalt nanoparticles can be synthesised using a modified version of the well-established synthetic route to smaller epsilon cobalt particles. Although polycrystalline, the particles are ferromagnetic at room temperature showing exchange bias on cooling. Particles have a large room temperature M_s ~131 emu/g and after initial exposure to air appear to be stable to further oxidation.

Oleic acid and trioctylphosphine oxide were the only surfactants used in this synthesis. The addition of co-surfactants was not required to produce particles of this type. Rather, by lowering the reaction temperature, not agitating the solution and ensuring there is not an excess of oleic acid, larger cubic particles formed. Our minor modification to the synthetic procedure highlights the complex nature of cobalt nanoparticle chemistry.

Acknowledgements

The authors would like to acknowledge Chevron, who through the Western Australian Research Alliance (WA:ERA) has financially supported the work. The authors acknowledge the facilities, and the scientific and technical assistance of the Australian Microscopy & Microanalysis Research Facility at the Centre for Microscopy, Characterisation & Analysis, The University of Western Australia, a facility funded by the University, State and Commonwealth Governments. ROF would like to thank the University of Western Australia for a UWA ReEntry Fellowship.

References

1. A.-H. Lu, W. Schmidt, N. Matoussevitch, H. Bönnemann, B. Spliethoff, B. Tesche, E. Bill, W. Kiefer and F. Schüth, *Angew. Chem. Int. Ed.*, 2004, **43**, 4303-4306.
2. N. Hondow and R. O. Fuller, *J. Coll. Inter. Sci.*, 2014, **417**, 396-401.
3. T. Hyeon, *Chem. Commun.*, 2003, 927-934.
4. J. N. Anker, W. P. Hall, O. Lyandres, N. C. Shah, J. Zhao and R. P. Van Duyne, *Nature Mater.*, 2008, **7**, 442-453.
5. A.-H. Lu, E. L. Salabas and F. Schüth, *Angew. Chem. Int. Ed.*, 2007, **46**, 1222-1244.
6. N. A. Frey, S. Peng, K. Cheng and S. Sun, *Chem. Soc. Rev.*, 2009, **38**, 2532-2542.
7. M. Colombo, S. Carregal-Romero, M. F. Casula, L. Gutierrez, M. P. Morales, I. B. Bohm, J. T. Heverhagen, D. Prosperi and W. J. Parak, *Chem. Soc. Rev.*, 2012, **41**, 4306-4334.
8. L. H. Reddy, J. L. Arias, J. Nicolas and P. Couvreur, *Chem. Rev.*, 2012, **112**, 5818-5878.
9. U. Jeong, X. Teng, Y. Wang, H. Yang and Y. Xia, *Adv. Mater.*, 2007, **19**, 33-60.
10. S. Sun and C. B. Murray, *J. Appl. Phys.*, 1999, **85**, 4325-4330.
11. K. M. Krishnan, *IEEE Trans. Magn.*, 2010, **46**, 2523-2558.
12. Q. A. Parkhurst, J. Connolly, S. K. Jones and J. Dobson, *J. Phys. D: Appl. Phys.*, 2003, **36**, R167-R181.
13. D. Kim, N. Lee, M. Park, B. H. Kim, K. An and T. Hyeon, *J. Am. Chem. Soc.*, 2008, **131**, 454-455.
14. T. Wang, X. Wang, D. LaMontagne, Z. Wang, Z. Wang and Y. C. Cao, *J. Am. Chem. Soc.*, 2012, **134**, 18225-18228.

15. L. T. Lu, L. D. Tung, I. Robinson, D. Ung, B. Tan, J. Long, A. I. Cooper, D. G. Fernig and N. T. K. Thanh, *J. Mater. Chem.*, 2008, **18**, 2453-2458.
16. C. P. Gräf, R. Birringer and A. Michels, *Phys. Rev. B*, 2006, **73**, 212401.
17. D. P. Dinega and M. G. Bawendi, *Angew. Chem. Int. Ed.*, 1999, **38**, 1788-1791.
18. V. F. Puntes, D. Zanchet, C. K. Erdonmez and A. P. Alivisatos, *J. Am. Chem. Soc.*, 2002, **124**, 12874-12880.
19. Y. Bao, W. An, C. H. Turner and K. M. Krishnan, *Langmuir*, 2010, **26**, 478-483.
20. F. Dumestre, B. Chaudret, C. Amiens, M.-C. Fromen, M.-J. Casanove, P. Renaud and P. Zurcher, *Angew. Chem. Int. Ed.*, 2002, **41**, 4286-4289.
21. F. Dumestre, B. Chaudret, C. Amiens, M. Respaud, P. Fejes, P. Renaud and P. Zurcher, *Angew. Chem. Int. Ed.*, 2003, **42**, 5213-5216.
22. A. Dreyer, M. Peter, J. Mattay, K. Eckstädt, A. Hütten and P. Jutzi, *Eur. J. Inorg. Chem.*, 2012, **2012**, 198-202.
23. C. Osorio-Cantillo, O. Perales-Perez and M. J. Guinel, *J. Appl. Phys.*, 2011, **109**, 07B531.
24. J. B. Tracy, D. N. Weiss, D. P. Dinega and M. G. Bawendi, *Phys. Rev. B*, 2005, **72**, 064404.
25. R. L. Stamps, *J. Phys. D: Appl. Phys.*, 2000, **33**, R247-R268.
26. V. Skumryev, S. Stoyanov, Y. Zhang, G. Hadjipanayis, D. Givord and J. Nogues, *Nature*, 2003, **425**, 850-853.
27. Y. Kang, J. B. Pyo, X. Xe, R. E. Diaz, T. R. Gordon, E. A. Stach and C. B. Murray, *ACS Nano*, 2013, **7**, 645-653.
28. B. W. Lee, R. Alsenz, A. Ignatiev and M. A. Van Hove, *Phys. Rev. B*, 1978, **17**, 1510-1520.
29. V. A. de la Peña O'Shea, I. d. P. R. Moreira, A. Roldán and F. Illas, *J. Chem. Phys.*, 2010, **133**, 024701.
30. V. F. Puntes, K. M. Krishnan and A. P. Alivistos, *Science*, 2001, **291**, 2115-2117.
31. A. C. S. Samia, K. Hyzer, J. A. Schlueter, C.-J. Qin, J. S. Jiang, S. D. Bader and X.-M. Lin, *J. Am. Chem. Soc.*, 2005, **127**, 4126-4127.
32. V. K. LaMer and R. H. Dinegar, *J. Am. Chem. Soc.*, 1950, **72**, 4847-4854.
33. X. Peng, J. Wickham and A. P. Alivisatos, *Journal of the American Chemical Society*, 1998, **120**, 5343-5344.
34. J. Gao, C. M. Bender and C. J. Murphy, *Langmuir*, 2003, **19**, 9065-9070.
35. Y. Bao, A. B. Pakhomov and K. M. Krishnan, *J. Appl. Phys.*, 2005, **97**, 10J317.
36. H. T. Yang, Y. K. Su, C. M. Shen, T. Z. Yang and H. J. Gao, *Surf. Inter. Anal.*, 2004, **36**, 155-160.
37. V. F. Puntes, K. M. Krishnan and P. Alivisatos, *Appl. Phys. Lett.*, 2001, **78**, 2187-2189.
38. M. Verelst, T. O. Ely, C. Amiens, E. Snoeck, P. Lecante, A. Mosset, M. Respaud, J. M. Broto and B. Chaudret, *Chem. Mater.*, 1999, **11**, 2702-2708.
39. D.-H. Ha, L. M. Moreau, C. R. Bealing, H. Zhang, R. G. Hennig and R. D. Robinson, *J. Mater. Chem.*, 2011, **21**, 11498-11510.
40. H. Zhang, D.-H. Ha, R. Hovden, L. F. Kourkoutis and R. D. Robinson, *Nano Letters*, 2010, **11**, 188-197.
41. P. A. Stadelmann, *JEMS - EMS java version*, 2004.
42. R. C. O'Handley, *Modern Magnetic Materials: Principles and Applications*, John Wiley and Sons, New York, 2000.
43. W. Hines, J. Budnick, D. Perry, S. Majetich, R. Booth and M. Sachin, *Phys. Status Solidi B*, 2011, **248**, 741-747.
44. G. Herzer, *IEEE Trans. Magn.*, 1990, **26**, 1397-1402.
45. M. E. McHenry, M. A. Willard and D. E. Laughlin, *Progress in Materials Science*, 1999, **44**, 291-433.
46. W. H. Meiklejohn and C. P. Bean, *Phys. Rev.* , 1957, **105**, 904-913.
47. J. Nogues and I. K. Schuller, *J. Magn. Magn. Mater.*, 1999, **192**, 203-232.
48. S. Sun, H. Zeng, D. B. Robinson, S. Raoux, P. M. Rice, S. X. Wang and G. Li, *Journal of the American Chemical Society*, 2004, **126**, 273-279.
49. T. Hyeon, S. S. Lee, J. Park, Y. Chung and H. B. Na, *Journal of the American Chemical Society*, 2001, **123**, 12798-12801.
50. C. Lofton and W. Sigmund, *Adv. Funct. Mater.*, 2005, **15**, 1197-1208.